Capture of solar and higher-energy neutrinos by ^{127}I

J. Engel
Deptartment of Physics and Astronomy, CB3255, University of North Carolina, Chapel Hill, North Carolina 27516

S. Pittel
Bartol Research Institute, University of Delaware, Newark, Delaware 19716

P. Vogel
Physics Department, 161-33, Caltech, Pasadena, California 91125
(Received 17 February 1994)

We discuss and improve a recent treatment of the absorption of solar neutrinos by ^{127}I, in connection with a proposed solar neutrino detector. With standard-solar-model fluxes and an in-medium value of -1.0 for the axial-vector coupling constant g_A, we obtain a ^{8}B-neutrino cross section of 3.3×10^{-42}, about 50% larger than in our previous work, and a ^{7}Be cross section that is less certain but nevertheless also larger than before. We then apply the improved techniques to higher incoming energies that obtain at the LAMPF beam dump, where an experiment is underway to finalize a calibration of the ^{127}I with electron neutrinos from muon decay. We find that forbidden operators, which play no role in solar-neutrino absorption, contribute nonnegligibly to the LAMPF cross section, and that the preliminary LAMPF mean value is significantly larger than our prediction.

PACS number(s): 96.60.Kx, 25.30.Pt, 21.60.−n

I. INTRODUCTION

In 1988 Haxton [1] proposed ^{127}I as the active ingredient in a new solar-neutrino detector. He estimated that a tank containing 1000 tons of iodine would detect about 20 times as many neutrinos as the chlorine experiment at Homestake. He also noted that a $3/2^+$ state at 125 keV in ^{127}Xe is accessible to neutrinos from ^{7}Be, and that if the ratio of ^{7}Be and ^{8}B cross sections were substantially different from that in chlorine, then the two experiments combined could determine the fluxes of both the ^{7}Be and ^{8}B neutrinos. Since the ^{7}Be flux now appears to be a critical piece of the solar-neutrino puzzle [2], a high-statistics iodine detector has become attractive.

In 1991 we attempted [3] to improve on Haxton's estimate by using the quasiparticle Tamm-Dancoff approximation (QTDA) to calculate the response of iodine to both ^{8}B and ^{7}Be neutrinos. We concluded that Haxton's estimate was a little too high, but our results were still sufficiently encouraging (and carried enough uncertainty) to make a direct calibration desirable. In fact, around the same time an attempt was made [4] to measure the Gamow-Teller (GT) strength distribution, which determines solar-neutrino cross sections, via the charge-exchange reaction ^{127}I$(p,n)^{127}$Xe. Unfortunately, in cases for which no states in the final nucleus are accessible by beta decay, the reaction determines the GT distribution only up to an overall normalizing constant. The solar neutrino cross section in ^{127}I can therefore not be extracted without measuring at least one more quantity—for example, the absolute GT strength to a particular state, or the total integrated strength below a certain energy.

To fix the normalization of the GT distribution, and to demonstrate that the counting of ^{127}Xe works as expected, a group working at LAMPF has recently exposed an iodine target to a known flux of electron neutrinos from muon decay [5]. The underlying idea is to use the total LAMPF cross section to fix the unknown constant multiplying the GT distribution. This task, unfortunately, is not completely straightforward. Because the LAMPF neutrinos have on average an energy of about 30 MeV, their wavelengths are short enough to change the form of the cross section; forbidden operators that depend on nucleon coordinates and momenta can modify the "allowed" strength from the GT operator $\sum_i \sigma_i \tau_i^+$. For the experiment to yield a reliable normalization, the forbidden contributions must either be small or accurately calculated and removed. The current state of affairs has prompted us to reexamine neutrino absorption by ^{127}I. Here, after reviewing our prior work in Sec. II and developing an improved version in Sec. III, we calculate the LAMPF cross section, including the forbidden corrections. These turn out to be large enough to complicate an accurate extraction of the allowed component from experimental data.

II. REVIEW OF PRIOR WORK

In Ref. [3] we developed an approximation for odd-mass nuclei that is closely related to the usual even-even QTDA. The starting point is the assumption that the ground state of ^{127}I is predominantly of one-quasiparticle character,

$$\pi^\dagger_{d_{5/2}} |\mathrm{BCS}\rangle , \tag{2.1}$$

where $|\mathrm{BCS}\rangle$ is the fully paired BCS quasiparticle vacuum and $\pi^\dagger_{d_{5/2}}$ creates a proton quasiparticle in the $1d_{5/2}$ orbit. We confirmed our assumption in part by adding three-quasiparticle states of the form

$$\left[\left(\pi_i^\dagger \nu_k^\dagger\right)^K \nu_l^\dagger\right]^{5/2} |\mathrm{BCS}\rangle\,, \tag{2.2}$$

the admixtures of which turned out to be small. (In the above equation i,k,l are valence orbitals and $\nu_l^\dagger$ creates a quasineutron in orbit l.) The form of the iodine ground state implies that the space of states in xenon accessible via neutrino absorption is largely spanned by the analogous set

$$\nu_j^\dagger |\mathrm{BCS}\rangle\,, \qquad \left[\left(\pi_i^\dagger \nu_k^\dagger\right)^K \pi_l^\dagger\right]^J |\mathrm{BCS}\rangle\,, \tag{2.3}$$

where J^π and j^π assume the values $3/2^+, 5/2^+$, and $7/2^+$, and K is any intermediate angular momentum. We therefore used the set Eq. (2.3) in calculating the ^{127}Xe spectrum and the GT strength distribution.

Our valence space for both protons and neutrons consisted of the $2s-1d-0g$ oscillator shell plus the two $0h$ orbitals from the next oscillator shell. We took the two-body interaction from Ref. [6] and modified it by scaling the pairing matrix elements to reproduce empirical pairing gaps and replacing the neutron-proton monopole-monopole component with a constant average interaction. We changed the monopole component because it alters single-particle energies through mean field effects, which we accounted for phenomenologically by taking our single-particle energies from a Wood-Saxon potential with parameters appropriate for ^{127}I. The end result of our calculation was (assuming standard-solar-model fluxes) a ^{8}B cross section of 2.2×10^{-42} (13 SNU) — smaller than Haxton's estimate by almost a factor of 3 — and a ^{7}Be cross section of $2.0\times10^{-45}\,\mathrm{cm}^2$ (9.4 SNU). The ratio of ^{7}Be to ^{8}B cross sections was much larger than in chlorine.

There were of course drawbacks in our approach. First of all, the QTDA is number-nonconserving; fluctuations in particle number introduce some error, which we were unable to estimate. In addition, we omitted basis states that might prove important despite the argument above. For example, three-quasineutron configurations in ^{127}Xe should combine with the states in Eq. (2.3) to create a low-lying collective 2^+ phonon, which could in turn modify the strength distribution at low excitation energies. In ^{127}I, a quadrupole phonon formed from three-quasiproton configurations plus the states in Eq. (2.2) could significantly dilute the one-quasiparticle content of the ground state. Furthermore, our two-body interaction was not entirely consistent with our selection of single-particle energies because we retained the like-particle monopole component while arguing that the neutron-proton monopole interaction ought to be excluded. Both can modify single-particle energies and, moreover, neither is trustworthy no matter how the energies are chosen (for a convincing demonstration see Ref. [7]). Finally, we took no account of spreading widths associated with our states in xenon. In revisiting our calculation we have addressed all these issues.

III. IMPROVED APPROACH

We have now improved our treatment of neutrino absorption by ^{127}I in several ways. To determine the error introduced by number-nonconservation in the QTDA, we have recalculated the GT distribution in the number-conserving Generalized-Seniority (GS) [8] approximation (which is equivalent to QTDA in all other respects). The one- and three-quasiparticle configurations above correspond to well-defined states in the GS approach. The comparison will be discussed in detail shortly.

We have also made several improvements to the effective force. For example, we have now removed the monopole component of the interaction both in the neutron-proton and like-particle channels, and have not replaced them with anything else. The average interaction that we included earlier has no effect (except on binding energies) in the number-conserving GS approach and so can be omitted. We argued previously that some remnant of the monopole force might be needed in a QTDA treatment, where because of the mixing of particle numbers even a constant interaction can change wave functions and energies. We now find, however, that the effects of number-nonconservation are minimized when the monopole force is dropped altogether. In addition, we no longer scale the like-particle interaction in the pairing channels. Although the scaling improves agreement with pairing gaps, it badly affects properties of low-lying states (e.g., energies and magnetic moments).

Beside altering the two-body interaction, we have also changed the way we select single-particle energies. In our earlier work, we used the energies given in Ref. [9]; here we take them instead from the spectra of $N=81$ nuclei (for neutrons) and $Z=51$ nuclei (for protons) that are close to ^{127}I and ^{127}Xe. The new single-particle energies yield a better ordering of low-lying levels in both mass-127 nuclei — the old ones reversed the order, e.g., of the $5/2^+$ and $7/2^+$ levels in ^{127}I. Another important change is the inclusion in the QTDA of the three-quasiproton and three-quasineutron configurations discussed above. And finally, we have now taken some account of the background of even more complex states by giving the final states a spreading width. Below we discuss all of these changes and their effects in detail.

In the GS approximation, the BCS vacuum is replaced by a number-conserving involving a condensate of $J=0$ S pairs for protons and a corresponding condensate for neutrons, viz.:

$$\begin{aligned} |w_p = w_n = 0\rangle &\equiv |N_p, N_n\rangle \\ &= (S_p^\dagger)^{N_p} (S_n^\dagger)^{N_n} |0\rangle\,, \end{aligned} \tag{3.1}$$

where $(\rho = p, n)$

$$S_\rho^\dagger = \sum_j (2j+1)^{\frac{1}{2}} \alpha_j^\rho \left[\rho_j^\dagger \rho_j^\dagger\right]^0 \tag{3.2}$$

creates a coherent $J=0$ pair, the state $|0\rangle$ contains no valence particles, N_p and N_n are the number of proton

and neutron valence S pairs, w_ρ denotes the generalized seniority for particles of type ρ, and the α_j^ρ are (variationally determined) structure constants related to the u_j's and v_j's of the BCS formulation. In this framework, our original QTDA treatment of xenon corresponds to diagonalizing the shell-model Hamiltonian in the space of states

$$|w_p = 0, w_n = 1\rangle = n_j^\dagger |N_p, N_n\rangle , \tag{3.3}$$

$$|w_p = 2, w_n = 1\rangle = \left[\left(p_i^\dagger p_l^\dagger\right)^K n_k^\dagger\right]^J |N_p - 1, N_n\rangle ,$$

where $n_j^\dagger$ and $p_j^\dagger$ now create *real* particles. An analogous construction yields the states in iodine corresponding to those in Eq. (2.2). (The one spurious state in each nucleus with $K = 0$ is easily removed.)

In Table I we display the energies of low-lying states, alongside those calculated in the GS and QTDA approximations (without three-like-quasiparticle states or their GS equivalents). Neither calculation does terribly well, but two facts are important. First, the two agree well with one another. Second, the calculations agree worst with experiment when three-quasiparticle configurations are important. This problem will partly be remedied later when we add the three-like-quasiparticle states.

Figure 1 shows the GT strength up to 8 MeV — the strength above 7.23 MeV, the neutron-emission threshold is irrelevant for *radiochemical* neutrino detection — calculated in the same two schemes. Here, as in Ref. [3], we have reduced the strengths by a phenomenological quenching parameter $(1.0/1.26)^2$. The validity of this simple prescription, which in weak interactions corresponds to setting g_A to -1.0, is not universally accepted and we will return to it later. For now we note the remarkable agreement between the two methods. The total strength below threshold is 4.38 in the GS calculation and 4.13 in the QTDA. The ^{8}B cross sections are 4.39×10^{-42} and 3.91×10^{-42}, respectively, close to one another but also markedly larger than that reported in Ref. [3] (the largest part of the change is due to the pairing matrix elements, which we no longer renormalize). The only important disagreement between the two calculations is in the strength to the lowest $3/2^+$ state: 0.079 in the GS scheme and 0.042 in the QTDA. Although it is unreasonable to expect calculations designed to reproduce the entire spectrum to match up state by state, in this instance the disagreement is disappointing because this one strength completely determines the cross section for ^{7}Be neutrinos. The GS strength is more than twice as large as in our previous paper (0.035) and, if correct, would (again with standard solar fluxes) result in more events from ^{7}Be than from ^{8}B. By comparison, the QTDA result for the first $3/2^+$ state is only marginally bigger than before. The GS calculation is clearly preferable since it does not violate particle number, but because of its complexity we have not extended it to include more configurations (which can also affect the ^{7}Be strength), as we have in the QTDA. We, therefore, cannot make a terribly strong statement about the ^{7}Be cross section; all signs, however, point to its being much larger with respect to the ^{8}B cross section than in ^{37}Cl. Other properties are very similar in the two approaches provided all monopole forces are set to zero. For the rest of this paper, then, we will no longer use the GS scheme, since the QTDA is computationally much simpler to extend.

We next examine the effects of the three-quasineutron and three-quasiproton configurations in the QTDA. Table II shows the same energy levels as in Table I, but with the extra configurations included. The result is a dramatic lowering in energy of some of the mainly three-quasiparticle states, reflecting the formation via the neutron-proton interaction of a collective quadrupole

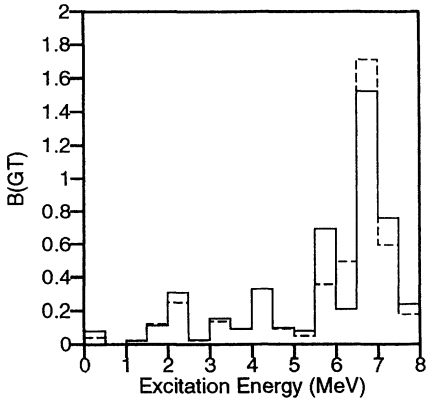

FIG. 1. The Gamow-Teller strength B(GT) (quenched and in half-MeV bins) from ^{127}I to states below 8 MeV in ^{127}Xe in the GS scheme (solid line) and in the QTDA (dashed line).

TABLE I. Energies of low-lying states in ^{127}I and ^{127}Xe in keV. The second column contains measured values, the third the QTDA predictions, and the last the GS predictions. Neither calculation incorporates three-like-quasiparticle states (or their analogs in the GS scheme).

	J^π	Expt.	QTDA	GS
^{127}I				
	$5/2^+$	0	0	0
	$7/2^+$	58	−14	62
	$3/2^+$	203	1261	1407
	$1/2^+$	375	1171	1299
	$5/2^+$	418	1695	1929
^{127}Xe				
	$1/2^+$	0	0	0
	$3/2^+$	125	178	300
	$9/2^-$	297	1449	1590
	$11/2^-$	309	−16	80
	$3/2^+$	322	1351	1430
	$7/2^+$	346	853	860
	$5/2^+$	376	1009	970
	$1/2^+$	412	1530	1430
	$5/2^+$	510	1428	1560
	$3/2^+$	587	1616	1720
	$9/2^+$	646	1588	1630

TABLE II. Energies of low-lying states in ^{127}I and ^{127}Xe in keV. The second column reprises the measured energies and the third column contains the predictions of the QTDA with three-like-quasiparticle configurations included. They should be compared with the results of the simpler QTDA calculation in Table I.

	J^π	Expt.	QTDA (improved)
^{127}I			
	$5/2^+$	0	0
	$7/2^+$	58	67
	$3/2^+$	203	636
	$1/2^+$	375	941
	$5/2^+$	418	555
^{127}Xe			
	$3/2^+$	125	216
	$9/2^-$	297	360
	$11/2^-$	309	153
	$3/2^+$	322	547
	$7/2^+$	346	630
	$5/2^+$	376	367
	$1/2^+$	412	898
	$5/2^+$	510	664
	$3/2^+$	587	682
	$9/2^+$	646	1528

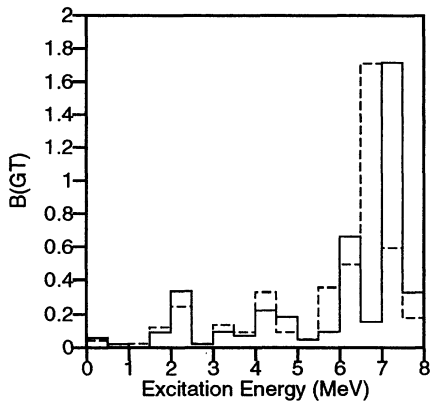

FIG. 2. The Gamow-Teller strength B(GT) (quenched and in half-MeV bins) from ^{127}I to states below 8 MeV in ^{127}Xe in the QTDA, with three-like-quasiparticle configurations included (solid line), and without them (dashed line — same as in Fig. 1).

phonon. The new configurations also increase the density of low-lying states substantially. Although the quantitative agreement in the lowest states is still not impressive, these new results are a considerable improvement. Furthermore, as noted above, the method is designed to encompass the entire final-state spectrum (in our model space several thousand states); the lowest-lying states, with the exception of the first $3/2^+$, are no more important than the others.

The formation of phonon-like states shifts the $E2$ strength downwards, although no single multiplet is as collective as implied by experiment. This may be an indication that further correlations associated with higher quasiparticle number (or with deformation) ought to be included at some level. The same conclusion might be drawn from the ^{127}I ground-state magnetic moment, which changes (with free g factors) from 4.39 to 3.76. (The experimental value is 2.81 and the Schmidt value is 4.79.) The incomplete but still significant improvement implies that spin correlations, important for parts of the GT distribution, are represented better than before, though again not perfectly. It also suggests that at least some extra quenching of the spin operator is in order.

In Fig. 2 we compare the QTDA GT strength below the neutron-emission threshold with and without the three-like-quasiparticle configurations. The difference, while non-negligible, is not dramatic. The low-lying phonon-like states apparently do little to the charge-changing strength, which is in a different channel. The main effect, a small overall loss of strength, is due largely to the reduction of the single-quasiparticle component of the ^{127}I ground-state from 86% to 76%. The ground-state three-quasiparticle components go mainly into *five-*quasiparticle states in ^{127}Xe, which are not included in our basis. To the extent that these states lie below the neutron-emission threshold (they should begin at roughly 4 times the pairing gap — about 4–5 MeV), we will underestimate the ^{8}B cross section. Phase space considerations reduce the importance of states this high in energy, however; in this application, therefore, the error should be relatively small.

The final new element in this paper is the inclusion of spreading widths. These depend on the density of complicated background states and on the average interaction strength coupling them to our model space, neither of which we can reliably estimate. We settle instead for the prescription in Ref. [10], developed primarily to describe spreading of RPA-like states high in energy, viz.:

$$\Gamma(\omega) \approx \frac{1}{\omega}\int_0^\omega d\epsilon\,[\gamma(\epsilon)+\gamma(\epsilon-\omega)]\,,$$
$$\gamma(\epsilon) = 10.75\left(\frac{\epsilon^2}{\epsilon^2+18^2}\right)\left(\frac{110^2}{\epsilon^2+110^2}\right), \qquad (3.4)$$

where ω is the excitation energy, $\gamma(\epsilon)$ is a parametrization of the single-quasiparticle width (in MeV), and we have included a lower limit of 300 keV to simulate experimental resolution. Figure 3 shows the full GT distribution with the widths included (and divided by 0.76 *in the figure only* to account for the strength in five-quasiparticle states, so that the height of the giant resonance is roughly correct). The spreading turns out to have a fairly small effect on both the total strength below threshold and the ^{8}B cross section. Our final values for these quantities, with all the new physics included and the spin operator quenched as discussed above, are 3.00 and 3.27×10^{-42}, respectively. The ^{8}B cross section is 50% larger than our old value. Using the free-nucleon axial-vector coupling constant would increase it another 60% and we can take that figure as a nominal measure of uncertainty in our result.

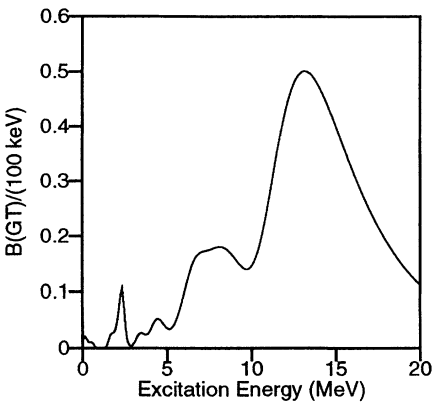

FIG. 3. The Gamow-Teller strength distribution B(GT) per 100 keV (quenched) from ^{127}I in the QTDA, with three-like-quasiparticle configurations and spreading widths included. The curve, which here goes up to 20 MeV in ^{127}Xe, has been scaled by 1/.76 to account for missing five-quasiparticle states lying largely in the giant resonance.

IV. HIGHER-ENERGY NEUTRINOS AND FORBIDDEN CORRECTIONS

Our strength distribution does not differ dramatically from the one extracted from experiment [4]. Both suffer from uncertainty in the overall normalization, which, as discussed in the Introduction, has prompted an attempt at LAMPF [5] to measure the total cross section for absorbing electron neutrinos from muon decay. But the energies of these neutrinos extend to half the muon mass, much higher than the solar neutrino end point ($\approx$ 14 MeV), and the momenta transferred are typically on the order of the inverse radius of the target nuclei. The allowed approximation, which ignores variations in the lepton wave functions over the interior of the nucleus, no longer applies and the cross section depends on nuclear wave functions in a more complicated way. Reference [11] contains a framework for treating neutrino-induced reactions beyond the allowed approximation; it involves calculating matrix elements of the operators:

$$\begin{aligned} &j_J(qr)Y_J(\Omega_r) \\ &j_L(qr)\,[Y_L(\Omega_r)\,\vec{\sigma}]^J \\ &j_L(qr)[Y_L(\Omega_r)\,\tfrac{1}{M}\vec{\nabla}]^J \\ &j_J(qr)Y_J(\Omega_r)\,\vec{\sigma}\cdot\tfrac{1}{M}\vec{\nabla}, \end{aligned} \tag{4.1}$$

where q is the momentum transfer, $j_L(qr)$ is the Lth spherical Bessel function, $Y_L(\Omega_r)$ is a spherical harmonic, J is the multipole order of the transition, and M is the nucleon mass. The maximum value of qr is about 2.8 and we need not consider multipoles above $J \approx 3$.

With our QTDA wave functions, the evaluation of the beam-dump cross section is nominally straightforward, but a few subtleties complicate the analysis. The most important difficulty arises in connection with the Coulomb attraction of the outgoing electron towards the $Z = 54$ xenon nucleus. In both the low-energy ($qr \ll 1$) [12] and high-energy ($qr \gg 1$) [13] limits, clear procedures exist for evaluating Coulomb effects; in one case the outgoing electron is known to be in an s state, enhancing the cross section by the usual Fermi factor, and in the other the outgoing wave function can be treated as a plane wave perturbed slightly by the charge distribution in the nuclear interior. Since $qr \approx 1$ here, neither limit applies and so we follow a different line of reasoning.

The multipolarity of the nuclear transition must be equal to that obtained from coupling the incoming and outgoing lepton angular momenta and parities. As we shall show shortly, the most important transitions have multipole quantum numbers 1^+ and 2^-. For 1^+ transitions, the orbital angular momenta of the two leptons must be coupled to either 0 or 2. The latter possibility requires both the neutrino and the electron to have $l = 1$ (or for one of them to have $l = 2$), which for the energies of interest here is less likely than the other possibility — that they both have $l = 0$, i.e., they are both in s states. We, therefore, treat Coulomb effects in the 1^+ channel as if the transitions were purely allowed — that is, we multiply the 1^+ cross section by the usual Fermi function $F(Z, E)$.

The 2^- transitions require at least one lepton to be in a $l = 1$ (or higher) state, and the usual prescription makes less sense. These are "unique" transitions, however, and can be treated simply in processes such as beta decay [14,15], for which qr is always small. The procedure there is to modify the usual cross section (with Fermi function) by a factor

$$\frac{p_\nu^2 + \lambda_2 p_e^2}{p_\nu^2 + p_e^2}, \tag{4.2}$$

where p_ν and p_e are the neutrino and electron momenta, respectively, and λ_2 is a function of p_e tabulated in Ref. [12]. Although qr is not always small enough in our problem for the procedure to be strictly valid, we employ it to get a rough handle on the Coulomb corrections; they turn out to add very slightly to the corrections produced by the Fermi function.

A less tractable issue is the proper value of g_A. Its effective reduction is believed to arise from quenching of the spin operator by complicated nuclear configurations outside typical model spaces (including ours). Even if our prescription for the GT strength is correct, it is far from clear that the higher multipoles should be affected in precisely the same way. We have, therefore, calculated the contribution of each multipole to the beam-dump cross section twice, using $g_A = -1.0$ and -1.26, with the idea that the true renormalization of each contribution probably lies somewhere in between.

The results, shown in Table III, reflect several effects. The presence of the Bessel functions in the second, third, and fourth operators in Eq. (4.1), and of q/M in the third and fourth operators, together reduce the 1^+ contribution to about 2/3 of its allowed value. (The Bessel-function effects can be computed reliably; in fact, the same calculation in the simple Helm model [16] gives a very similar result.) The contributions of the 2^+ and 3^+ operators, in which j_2 is the first Bessel function to appear, are nominally suppressed by the upper limit in

TABLE III. Contributions of individual multipoles to the total cross section for neutrinos from muon decay, in units of 10^{-40} cm^2. The two columns correspond to quenched and free values for g_A, respectively (see text).

J^π	$g_A = -1.0$	$g_A = -1.26$
0^+	0.096	0.096
0^-	0.00001	0.00002
1^+	1.017	1.528
1^-	0.006	0.008
2^+	0.155	0.213
2^-	0.693	1.055
3^+	0.149	0.171
3^-	0.017	0.025
Total	2.098	3.096

qr but are in fact far from negligible. The 0^+, on the other hand, contributes little even though it is unsuppressed because its strength is concentrated in the isobar analog state, which lies several MeV above the neutron-emission threshold. The 0^- and 1^- strengths are even more concentrated — within the giant-dipole resonance and its spin analog, well above 7.23 MeV. In fact, the 2^- contribution, which we find to be of the same order as that of the 1^+, may well be smaller than in our table, because the associated strength is probably also concentrated at higher energies. Our model space is clearly not large enough for the full collectivity of the spin-dipole mode to assert itself.

To get some idea of the size of our overestimate we performed QRPA calculations for ^{128}Xe with the same single-particle levels and effective interaction we used in the odd-mass nuclei. We then enlarged the model space to include the $1f$ and $2p$ levels a few MeV above the Fermi surface. We found that while the total 2^- strength increased, the amount below 7 MeV fell by 20–30 %. Including other levels below the Fermi surface (e.g., the $0f - 1p$ shell) would concentrate it still further; just how much would remain below threshold is not clear.

Altogether, the cross section for muon-decay neutrinos is only about half of the preliminary experimental value of 6×10^{-40} cm^2 [5], even without any quenching of the axial current. There is no clear way to make our results compatible with this larger cross section. As is apparent from the table, the bulk of the cross section comes from the 1^+ and 2^- multipoles, and we have argued that the 2^- contribution is probably an overestimate. Because the average neutrino energy is so much higher than 7 MeV, phase space plays only a small role and the GT 1^+ contribution depends essentially only on the total strength below the neutron-emission threshold — it is insensitive to the precise distribution. To account for the difference between our calculated total cross section and a value of 6×10^{-40} cm^2, the 1^+ contribution would have to be about three times larger than in Table III. An increase of about 25% might be plausible since, as discussed in connection with Fig. 3, we have not included states with five or more quasiparticles. Our claim, however, is that such states appear in large numbers only at energies above 4–5 MeV and that relatively few will contribute to the strength below threshold. In our calculation the summed GT strength below threshold is about 10% of the total strength, which is dominated ($\approx$ 70%) by the states that form the giant GT resonance at 13–14 MeV. Such a distribution is consistent with general experience in other nuclei; in fact it seems impossible to increase the low-lying GT strength substantially as long as the giant GT resonance is at the energy suggested by the (p,n) reaction, which in turn is in reasonable agreement with our calculation. Finally, though it is not impossible that we are seriously underestimating the contributions of the other multipoles, that would not be good news either. A forbidden contribution even larger than our estimate would make an extraction of the GT distribution extremely difficult. Unfortunately, therefore, we cannot reconcile our results with the value 6×10^{-40} cm^2 without invoking an unforeseen mechanism that would probably spoil the calibration.

V. CONCLUSIONS

In summary, we have recalculated cross sections for the capture by ^{127}I of neutrinos from solar ^{8}B and ^{7}Be decay — incorporating several new physical effects — and have found somewhat larger values than in our previous work. The physics we still have not included, e.g., further correlations/deformation, a precisely determined and justified value for g_A, a more carefully crafted interaction, etc., make our results somewhat uncertain, but with enough effort more comprehensive calculations are possible. Our current results, we feel, still support the development of a calibrated iodine-based solar-neutrino detector if only because it would be an improved version of the existing Homestake experiment, which as of now is the most difficult to reconcile with standard-model physics. We must also conclude, unfortunately, that a complete calibration may be more difficult than originally hoped. We do not see how the preliminary LAMPF cross section can be due entirely to GT-like strength, and do not as yet know how to evaluate and remove the forbidden contributions with the required accuracy. Nonetheless, we are hopeful that with the steady advance of experimental techniques, nuclear-structure expertise, and computing power, the remaining problems can be overcome.

ACKNOWLEDGMENTS

We wish to acknowledge useful conversations with W.C. Haxton and K. Lande. This work was supported in part by the U.S. Department of Energy under grants DE-FG05-94ER40827 and DE-FG03-88ER40397, and by the National Science Foundation under grants PHY-9108011 and PHY-9303041.

[1] W.C. Haxton, Phys. Rev. Lett. **60**, 768 (1988).
[2] J. Bahcall and H. Bethe, Phys. Rev. D **47**, 1298 (1993).
[3] J. Engel, S. Pittel, and P. Vogel, Phys. Rev. Lett. **67**, 426 (1991).
[4] E. Sugarbaker (private communication).
[5] B.T. Cleveland, T. Daily, J. Distel, K. Lande, C.K. Lee *et al.*, in *Proceedings of the 23rd International Cosmic Ray Conference* (University of Calgary, Alberta, Canada, 1993), Vol. 3, p. 865.
[6] A. Hosaka, K.I. Kubo, and K. Toki, Nucl. Phys. **A444**, 76 (1985).
[7] A. Abzouzi, E. Caurier, and A.P. Zucker, Phys. Rev. Lett. **66**, 1134 (1991).
[8] I. Talmi, Nucl. Phys. **A172**, 1 (1971).
[9] K. Grotz, H.V. Klapdor, and J. Metzinger, Phys. Rev. C **33**, 1263 (1986).
[10] R.D. Smith and J. Wambach, Phys. Rev. C **38**, 100 (1988).
[11] J. D. Walecka, in *Muon Physics*, edited by V.W. Hughes and C.S. Wu (Academic, New York, 1975), Vol. 2, p. 113.
[12] H. Behrens and J. Jänecke, in *Numerical Tables for Beta Decay and Electron Capture, Landolt-Bornstein, New Series Group 1*, edited by K.H. Hellwege and H. Schopper (Springer, New York, 1969), Vol. 4.
[13] R. Rosenfelder, Ann. Phys. (N.Y.) **128**, 188 (1980).
[14] H. Schopper, *Weak Interactions and Nuclear Beta Decay* (North-Holland, Amsterdam, 1966).
[15] H. Behrens and W. Bühring, *Electron Radial Wave Functions and Nuclear Beta-decay* (Clarendon, Oxford, 1982).
[16] R.H. Helm, Phys. Rev. **104**, 1466 (1956).